[Supporting Information]

Two-dimensional Janus antimony chalcohalides for efficient energy conversion applications

Poonam Chauhan, Jaspreet Singh and Ashok Kumar[*]

Department of Physics, Central University of Punjab, VPO Ghudda, Bathinda, 151401, India

(June 1, 2024)

*Corresponding Author: ashokphy@cup.edu.in

Geometric structure and energetics
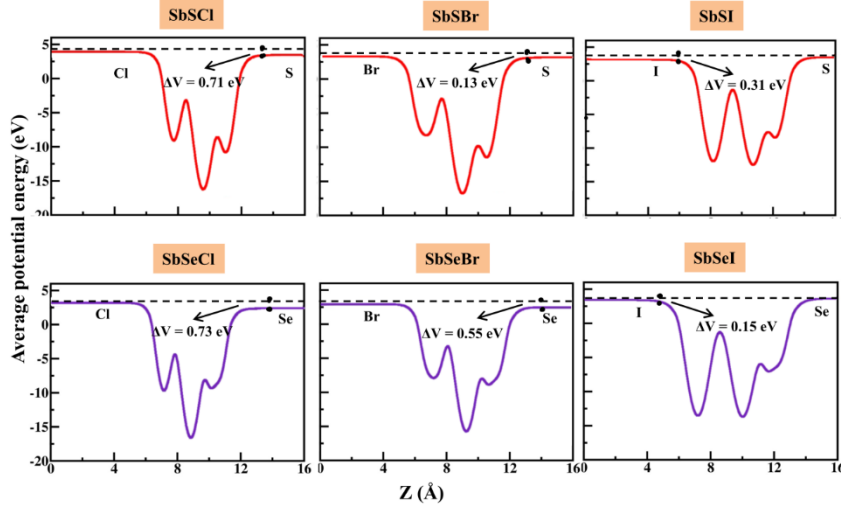
Fig. S1: Electrostatic potential curves of of SbYZ monolayers. The ΔV represents the potential difference between two sides of monolayers.

Thermal stability
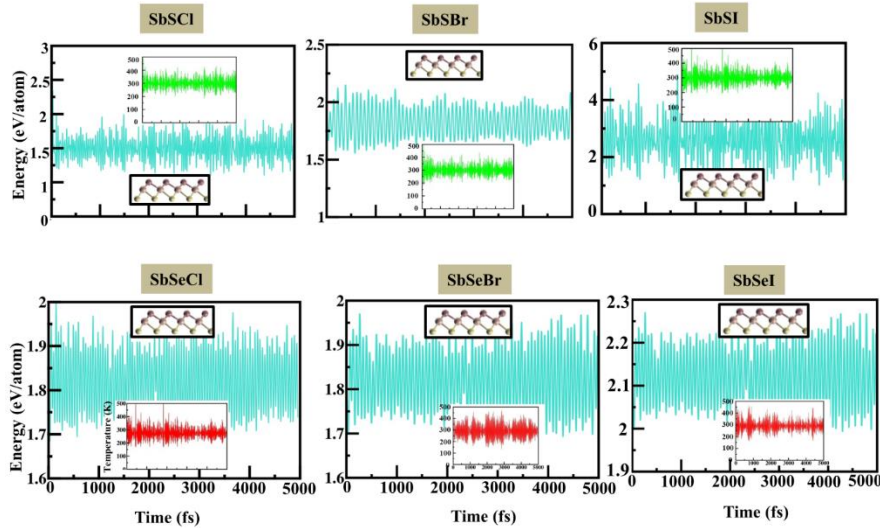
Fig. S2: The energy fluctuation as a function of time for Janus SbYZ monolayers at 300 K. The inset shows temperature fluctuation with time. The snapshots of the atomic configuration of SbYZ monolayers after 5ps are also shown.
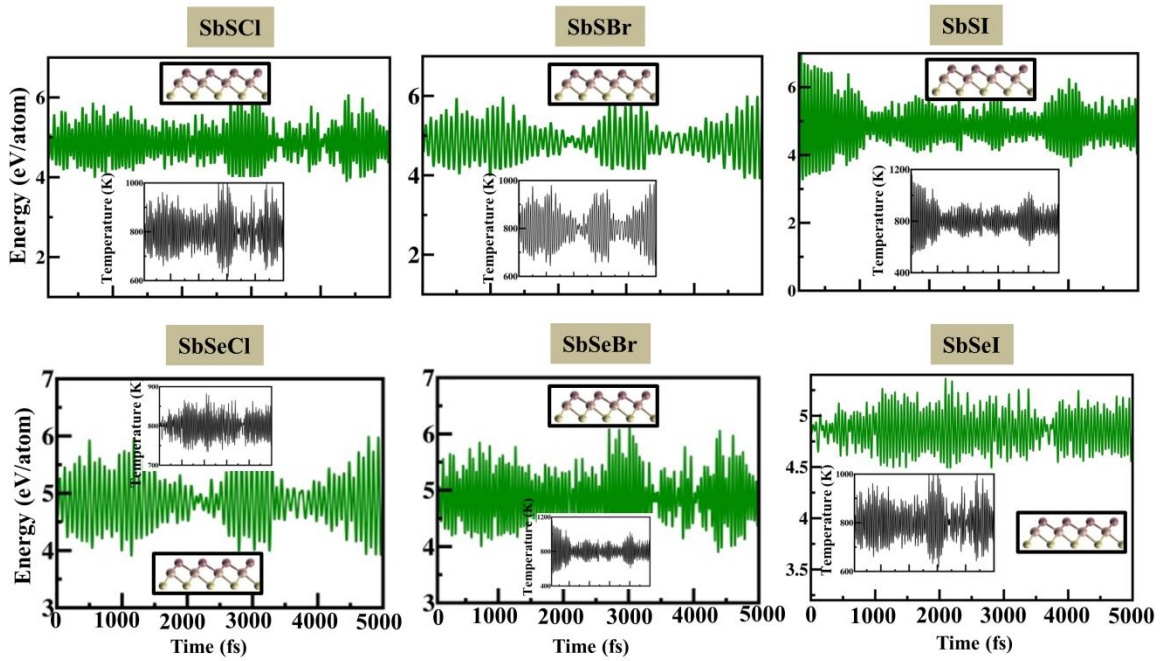
Fig. S3: The energy fluctuation as a function of time for Janus SbYZ monolayers at 800 K. The inset shows temperature fluctuation with time. The snapshots of the atomic configuration of SbYZ monolayers after 5ps are also shown.

Lattice thermal conductivity
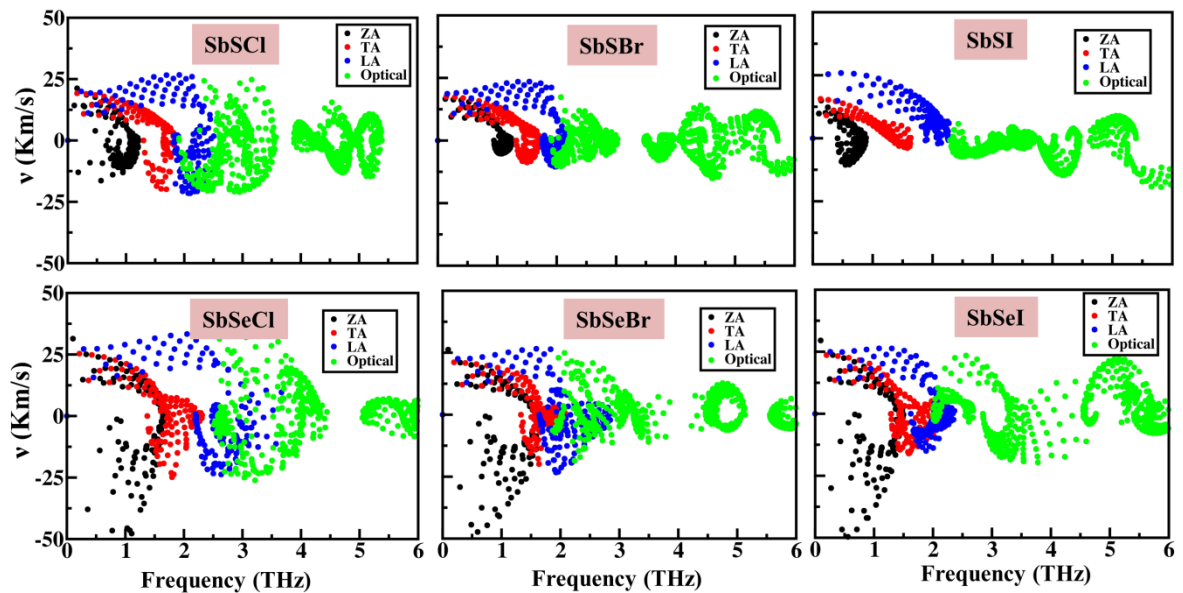
FIG. S4 Phonon group velocity (v_g) of 2D Janus SbYZ monolayers.
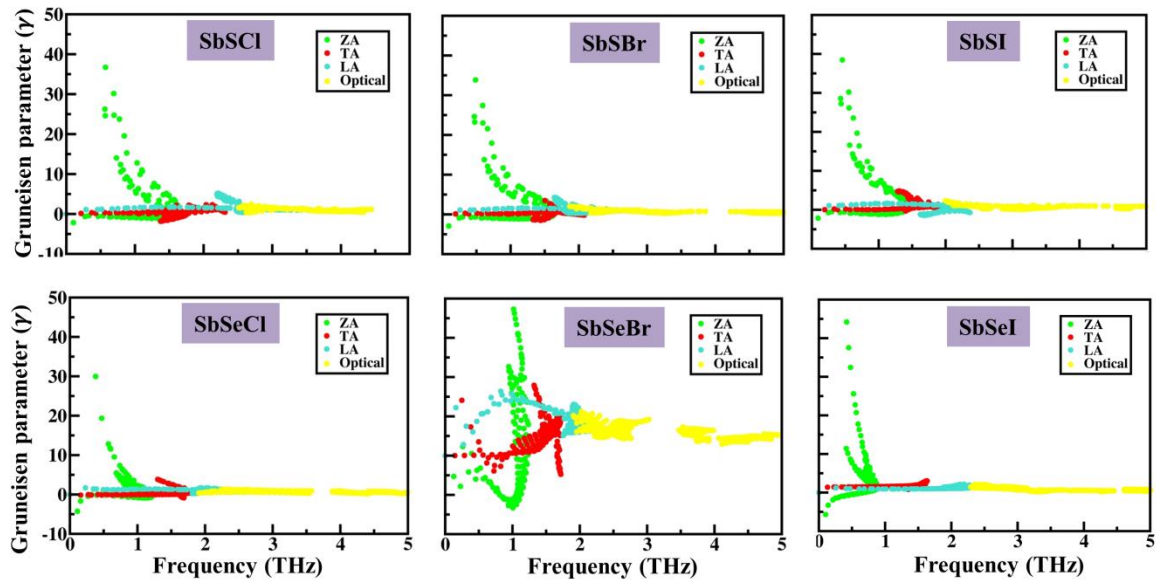
Fig. S5 Gruneisen parameter (γ) of 2D Janus SbYZ monolayers.

Magneto-transport properties
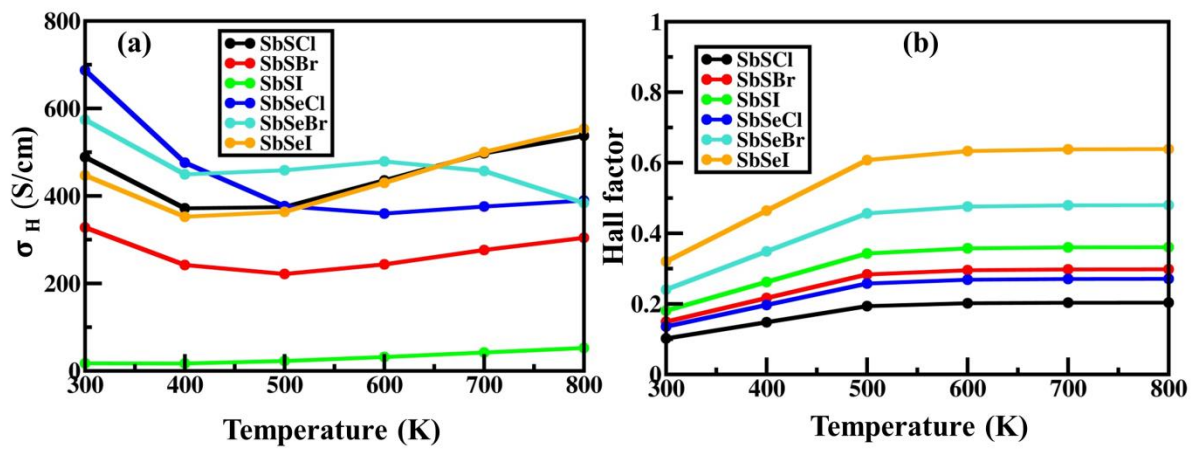
Fig. S6 (a) Hall conductivity and **(b)** Hall factor of 2D Janus SbYZ (Y= S, Se and Z= Cl, Br & I) monolayers.

Electronic structure

Table S1: The bandgap of 2D Janus SbYZ monolayers in eV using different level of theories. QP The quasi-particle (QP) direct bandgap and excitonic binding energy are also given.

2D monolayers	GGA	HSE06	G_0W_0	QP	E_b (eV)
SbSCl	1.42	2.04	2.53	3.17	0.87
SbSBr	1.39	1.97	2.46	3.14	0.80
SbSI	1.33	1.86	2.38	2.95	0.71
SbSeCl	1.37	1.92	2.41	3.12	0.82
SbSeBr	1.29	1.78	2.35	3.08	0.70
SbSeI	1.23	1.75	2.29	2.94	0.67

Scattering rate

The momentum-dependent relaxation time is calculated, including eight different kinds of scattering i.e., ionized impurity scattering ($\tau_{Ii}(k)$), polar optical phonon scattering ($\tau_{Pop}(k)$), dislocation scattering ($\tau_{Dis}(k)$), alloy scattering ($\tau_{Alloy}(k)$), intra-valley scattering ($\tau_{Iv}(k)$), piezoelectric scattering ($\tau_{Pz}(k)$), acoustic deformation scattering ($\tau_{Ac}(k)$) and neutral impurity scattering ($\tau_{Ni}(k)$), in the calculations.

Various scattering mechanisms for the calculation of relaxation time is expressed as [1-4]:

$$\frac{1}{Ii(k)} = \frac{e^4 N}{8\pi\varepsilon_0^2 \left(\frac{h}{2\pi}\right)^2 k^2 v(k)} \left[D(k)\ln\left(1 + \frac{4k^2}{\beta^2}\right) - B(k) \right] \tag{S1}$$

$$\frac{1}{\tau_{Ac}(k)} = \frac{e^2 k_B T \varepsilon_D^2 k^2}{3\pi\left(\frac{h}{2\pi}\right)^2 C_{el}\, v(k)} [3 - 8c^2(k) + 6c^4(k)] \tag{S2}$$

$$\frac{1}{\tau_{Pz}(k)} = \frac{e^2 k_B T P^2}{6\pi\varepsilon_0 \left(\frac{h}{2\pi}\right)^2 v(k)} [3 - 6c^2(k) + 4c^4(k)] \tag{S3}$$

$$\frac{1}{\tau_{Dis}(k)} = \frac{N_{dis}e^4 k}{\frac{h}{2\pi}^2 \varepsilon_0^2 C_l^2 v(k)} \frac{1}{\left(1+4\frac{k^2}{\beta^2}\right)^{3/2} \beta^4} \tag{S4}$$

$$\frac{1}{\tau_{Alloy}(k)} = \frac{3\pi k^2}{16\, v(k)\left(\frac{h}{2\pi}^2\right)} V_0 U_{alloy}^2 \chi(1-\chi) \tag{S5}$$

$$\frac{1}{\tau_{Iv}(k)} = (N_e + 1 - f^-)\lambda_e^- + (N_e + f^+)\lambda_e^+ \tag{S6}$$

$$\frac{1}{\tau_{Ni}(k)} = \frac{80\pi\varepsilon\left(\frac{h}{2\pi}\right)v(k)^2 N_n}{e^2 k^2} \tag{S7}$$
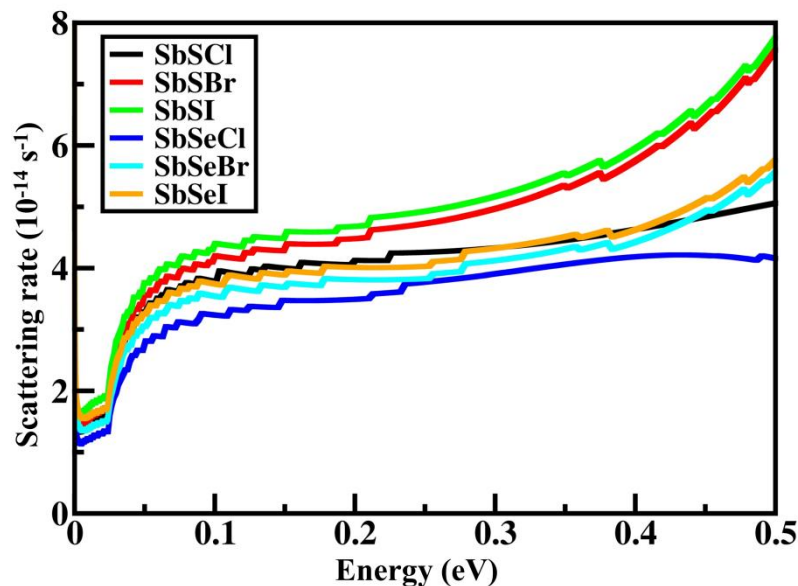
Fig. S7 Momentum dependent scattering rate of 2D Janus SbYZ monolayers including various scattering mechanism.
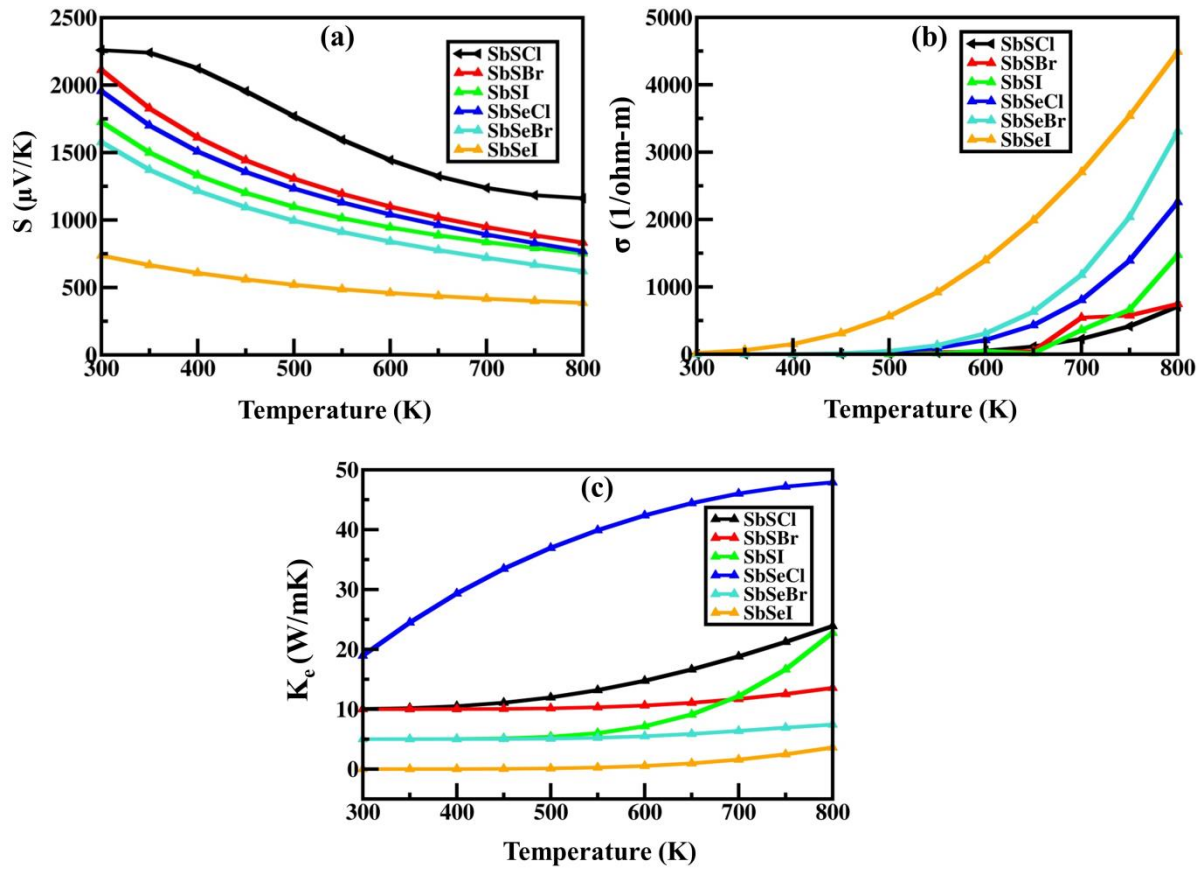
Fig. S8 (a) Seebeck coefficient (S) and (b) electrical conductivity (σ) and (**c**) electronic thermal conductivity (k_e) of 2D Janus SbYZ monolayers as a function of temperature.

Photovoltaic solar cell properties

Table S2 Lattice mismatch (%), conduction band-offset (ΔEc) corresponding to chalcogen sides and power conversion efficiencies (PCEs) of 2D Janus SbYZ monolayers constituting heterojunction solar cells. The ΔEc values in brackets corresponds to the halogen side of Janus SbYZ monolayers.

| Heterojunctions	Lattice Mismatch (%)	ΔEc (eV)	PCE (%)
SbSCl/AsTeCl	0.25	0.06	8.25
SbSCl/AsTeBr	1.01	0.3	10.63
SbSCl/β-Te$_2$S	3.48	1.0	10.76
SbSCl/BiSF	0.24	0.04	10.89
SbSBr/BiSBr	2.95	0.01	17.84
SbSBr/BiTeF	3.92	0.57	6.61
SbSBr/AsTeCl	1.52	0.46	9.12
SbSBr/AsTeBr	0.25	0.51	11.44
SbSBr/BiSF	1.0	0.56 (0.17)	12.73
SbSBr/AsTeI	2.25	0.25	16.50
SbSBr/BiSeBr	4.87		7.21
SbSI/BiSBr	0.98	0.56	11.56
SbSI/BiSCl	0.25	0.33	12.52
SbSI/BiSeCl	1.95	0.15	17.54
SbSI/BiSF	3.24	0.32	11.59
SbSeCl/SbSCl	2.26	0.32	12.54
SbSeCl/BiSeCl	2.92	0.21	16.71
SbSeCl/BiSBr	1.96	0.15	16.20
SbSeCl/BiSCl	0.73	0.33	12.53
SbSeCl/SbSeBr	1.48	0.13	17.65
SbSeCl/AsTeBr	1.25	0.28	14.97
SbSeCl/β-Te$_2$S	1.22	0.14	13.31
SbSeCl/AsTeI	1.48	0.19 (0.48)	17.19
SbSeBr/SbSBr	2.48	0.27 (0.31)	13.71
SbSeBr/SbSeCl	1.48	0.13 (0.23)	15.83
SbSeBr/SbSCl	3.73	0.45 (0.12)	14.39
SbSeBr/BiSCl	0.74	0.46	11.37
SbSeBr/AsTeCl	3.99	0.19 (0.06)	11.50
SbSeBr/AsTeBr	2.73	0.15 (0.18)	15.23
SbSeBr/AsTeI	0.24	0.35	19.10
SbSeBr/β-Te$_2$S	0.23	0.14	14.34

Table S3 PCEs of SbYZ heterojunction solar cell and other previously reported 2D heterojunction solar cell.

| Heterostructures	PCEs	References
SbSeBr/AsTeI	19	This study
CBN/PCBN	10 to 20	[5]
g-SiC$_2$/GaN bilayer	12 to 20	[6]
P-PdSe$_2$/MoTe$_2$	17	[7]
MoS$_2$/bilayer phosphorene	16-18	[8]
MoSe$_2$/ψ-phosphorene	20.26	[9]
GeSe/SnSe	21.47	[10]
β-Te$_2$Se(Se-Side)/H-MoSe$_2$	16.18	[11]
SbTeBr/SbSI	8.3%	[12]

Photocatalytic water splitting

The SbSI and SbSeCl monolayers can be oxidized and reduced by photogenerated charge carriers i.e. electrons and holes. The reduction and oxidation mechanism of SbYZ (Y = S and Se; Z = I and Br) monolayers are given as:

Reduction:

$$2SbYZ + 3H_2 \rightarrow 2Sb + 2H_2Y + 2HZ \tag{S8}$$

Oxidation:

$$2SbYZ + 2H_2O \rightarrow 2Y + 2Z + 2SbO + 2H_2 \tag{S9}$$
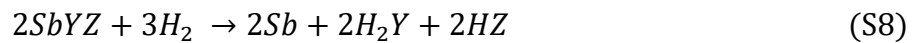
The thermodynamic reduction (ϕ^{re}) and oxidation potential of AsTeX (ϕ^{ox}) monolayers can be calculated as:

$$\phi^{re} = -\left[2\Delta_f G^0(Sb) + 2\Delta_f G^0(H_2Y) + 2\Delta_f G^0(HZ) - 2\Delta_f G^0(SbYZ) - 3\Delta_f G^0(H_2)\right]/$$

$$4eF + \phi(H^+ + H_2) \tag{S10}$$

$$\phi^{ox} = \left[2\Delta_f G^0(Y) + 2\Delta_f G^0(Z) + 2\Delta_f G^0(SbO) + 2\Delta_f G^0(H_2) - 2\Delta_f G^0(SbYZ) - 2\Delta_f G^0(H_2O)\right]/4eF + \phi(H^+ + H_2) \tag{S11}$$

The calculated values of ϕ^{re} and ϕ^{ox} is -1.41 eV (-1.27 eV) and 3.62 eV (3.61 eV) corresponding to SbSI (SbSeBr) monolayers.

Gibbs free energy profiles

We implemented the hydrogen electrode model for the evaluation of the Gibbs free energy change in water radox reactions i.e. given as:

$$\Delta G = \Delta E + \Delta E_{ZPE} - T\Delta S + \Delta G_U + \Delta G_{pH} \tag{S12}$$

$\Delta G_U = -eU$ and ΔG_{pH} (= $K_B T \times \ln 10 \times pH$)

Where T stands for temperature (298 K), ΔE for adsorption energy, ΔE_{ZPE} and ΔS are the difference in the zero-point energy and entropy. The free molecules (H_2, H_2O) entropies are taken from NIST database (https://cccbdb.nist.gov/). The calculated values of above parameters mentioned in Table S4.

The two-steps HER mechanism is given as:

$$* + H^+ + e^- \rightarrow *H \tag{i}$$

$$*H \rightarrow * + H_2 \tag{ii}$$

The free energy change for each intermediate steps of HER is determined by:

$$\Delta G_a = G(*H) - G(*) - G(H^+ + e^-) + \Delta G_U + \Delta G_{pH} \tag{S13}$$

$$\Delta G_b = G(*) - G(H_2) - G(*H) + \Delta G_U + \Delta G_{pH} \tag{S14}$$

Similarly the four steps OER process is illustrated as:

$$* + H_2O \rightarrow *OH + H^+ + e^- \tag{iii}$$

$$*OH \rightarrow *O + H^+ + e^- \tag{iv}$$

$$*O + H_2O \rightarrow *OOH + H^+ + e^- \tag{v}$$

$$* OOH \rightarrow * + O_2 + H^+ + e^- \qquad (vi)$$
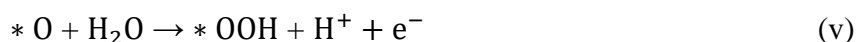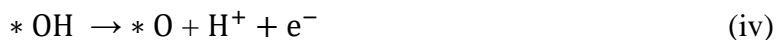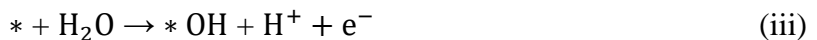
The free energy change for each intermediate steps of OER is determined by:

$$\Delta G_c = G(* OH) + G(H^+ + e^-) - G(*) - G(H_2O) + \Delta G_U - \Delta G_{pH} \qquad (S15)$$

$$\Delta G_d = G(* O) + G(H^+ + e^-) - G(* OH) + \Delta G_U - \Delta G_{pH} \qquad (S16)$$

$$\Delta G_e = G(* OOH) + G(H^+ + e^-) - G(* O) - G(H_2O) + \Delta G_U - \Delta G_{pH} \qquad (S17)$$

$$\Delta G_f = G(*) + G(H^+ + e^-) + G(O_2) - G(* OOH) + \Delta G_U - \Delta G_{pH} \qquad (S18)$$

The terms $G(O_2)$ and $G(H^+ + e^-)$ mentioned in above equations are calculated as; $2G(H_2O)$ $- 2G(H_2) + 4.92$ and $1/2G(H_2)$, respectively.

Table S4 Zero point energy correction (E_{ZPE}) and entropy of molecules and absorbants on SbSI (SbSeBr) monolayer.

| Species	E_{ZPE} (eV)	-TS (eV)
H₂	0.31 (0.28)	-0.41
H₂O	0.67 (0.57)	-0.67
*	-	-
*O	0.006 (0.004)	0.00
*OH	0.24 (0.23)	0.00
*OOH	0.40 (0.40)	0.00
*H	0.002 (0.003)	0.00
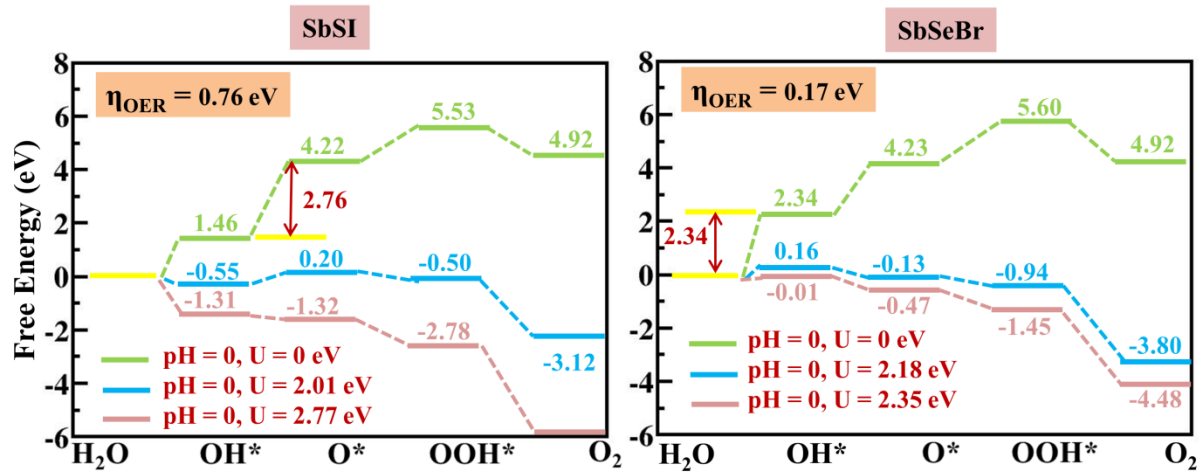
Fig. S9 The free energy change pathways for oxygen evolution reaction (OER) for SbSI and SbSeBr monolayers, respectively. The presence and absence of light irradiation is represented by green and sky blue lines, while a purple line represents extra potential required to make OER feasible.

Table S5 Corrected STH efficiency of Janus SbSI and SbSeBr monolayers and their comparison with other Janus monolayers in literature.

2D monolayers	STH (%)	References
SbSI, SbSeBr	12, 18	Our study
AsTeCl, AsTeBr	16, 10	[13]
MoSSe	15.46	[14]
WSSe	11.68	[15]
β-Te$_2$S, β-Te$_2$Se	13.46, 12.09	[11]
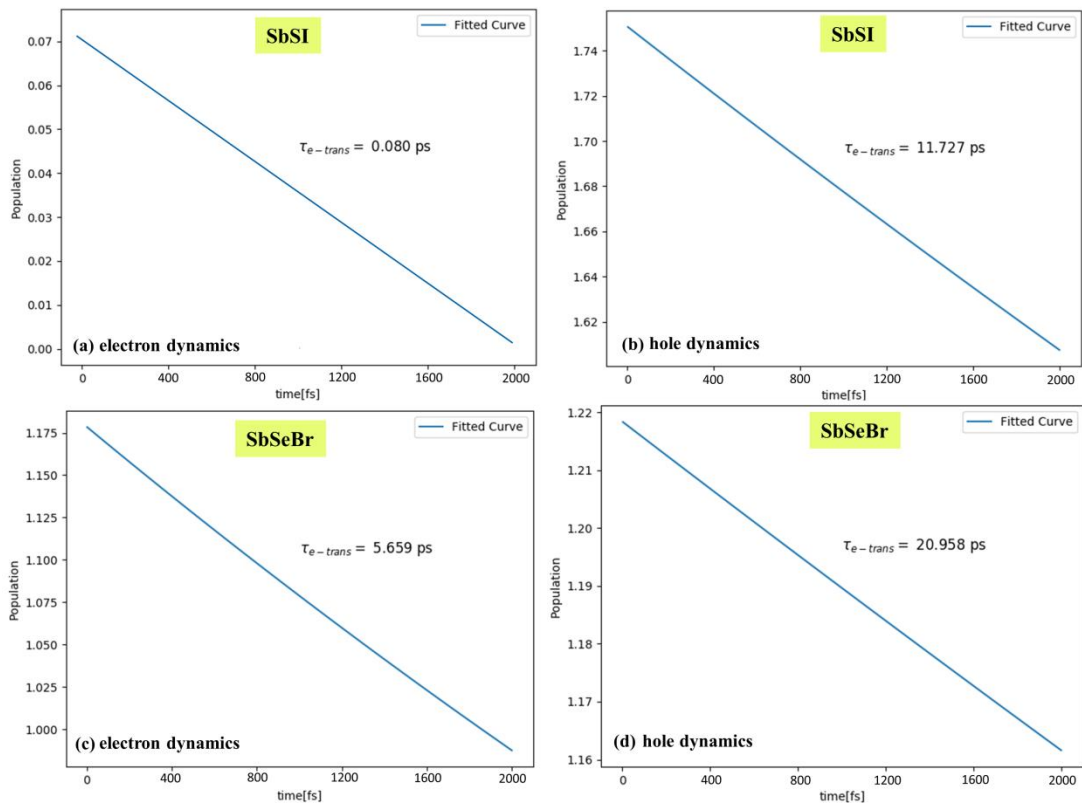
Fig. S10 The electron and holes dynamics of 2D Janus SbSI and SbSeBr monolayers.

References

1. A. Faghaninia, J. W. Ager III and C. S. Lo, *Physical Review B*, 2015, **91**, 235123.

2. N. Miller, E. E. Haller, G. Koblmüller, C. Gallinat, J. S. Speck, W. J. Schaff, M. E. Hawkridge, K. M. Yu and J. W. Ager III, *Physical Review B*, 2011, **84**, 075315.

3. A. T. Ramu, L. E. Cassels, N. H. Hackman, H. Lu, J. M. Zide and J. E. Bowers, *Journal of Applied physics*, 2010, **107**.

4. C. Erginsoy, *Physical Review*, 1950, **79**, 1013.

5. M. Bernardi, M. Palummo and J. C. Grossman, *ACS nano*, 2012, **6**, 10082-10089.

6. L.-J. Zhou, Y.-F. Zhang and L.-M. Wu, *Nano letters*, 2013, **13**, 5431-5436.

7. M. Jakhar, J. Singh, A. Kumar and R. Pandey, *The Journal of Physical Chemistry C*, 2020, **124**, 26565-26571.

8. J. Dai and X. C. Zeng, *The journal of physical chemistry letters*, 2014, **5**, 1289-1293.

9.   H. Wang, X. Li, Z. Liu and J. Yang, *Physical Chemistry Chemical Physics*, 2017, **19**, 2402-2408.

10.   Y. Mao, C. Xu, J. Yuan and H. Zhao, *Journal of Materials Chemistry A*, 2019, **7**, 11265-11271.

11.   J. Singh and A. Kumar, *Journal of Materials Chemistry C*, 2023.

12.   H.-y. Liu, H. Yang and Y. Zheng, *Physical Chemistry Chemical Physics*, 2024, **26**, 6228-6234.

13.   P. Chauhan, J. Singh and A. Kumar, *Journal of Materials Chemistry A*, 2023, **11**, 10413-10424.

14.   X. Ma, X. Wu, H. Wang and Y. Wang, *Journal of Materials Chemistry A*, 2018, **6**, 2295-2301.

15.   L. Ju, M. Bie, X. Tang, J. Shang and L. Kou, *ACS applied materials & interfaces*, 2020, **12**, 29335-29343.